Characterization of biochemical properties of a selenium-independent glutathione peroxidase of *Cryptosporidium parvum*

J.-M. KANG, H.-L. JU, W.-M. SOHN *and* B.-K. NA*

Department of Parasitology and Institute of Health Sciences, Gyeongsang National University School of Medicine, Jinju 660–751, Korea

(*Received 6 May 2013; revised 6 August and 9 September 2013; accepted 22 September 2013; first published online 13 December 2013*)

SUMMARY

Glutathione peroxidase (GPx; EC 1.11.1.9) is an important antioxidant enzyme that catalyses the reduction of organic and inorganic hydroperoxides to water in oxygen-consuming organisms, using glutathione as an electron donor. Here, we report the characterization of a GPx of *Cryptosporidium parvum* (CpGPx). CpGPx contained a standard UGU codon for cysteine instead of a UGA opal codon for seleno-cysteine (SeCys) at the active site, and no SeCys insertion sequence (SECIS) motif was identified within the 3′-untranslated region (UTR) of CpGPx, which suggested its selenium-independent nature. *In silico* and biochemical analyses indicated that CpGPx is a cytosolic protein with a monomeric structure. Recombinant CpGPx was active over a wide pH range and was stable under physiological conditions. It showed a substrate preference against organic hydroperoxides, such as cumene hydroperoxide and *t*-butyl hydroperoxide, but it also showed activity against inorganic hydroperoxide, hydrogen peroxide. Recombinant CpGPx was not inhibited by potassium cyanide or by sodium azide. The enzyme effectively protected DNA and protein from oxidative damage induced by hydrogen peroxide, and was functionally expressed in various developmental stages of *C. parvum*. These results collectively suggest the essential role of CpGPx for the parasite's antioxidant defence system.

Key words: *Cryptosporidium parvum*, glutathione peroxidase, selenium-independent glutathione peroxidase, drug target.

INTRODUCTION

Cryptosporidium parvum is an intracellular apicomplexa protozoan parasite, which primarily infects gastrointestinal epithelial cells of many vertebrates, including humans, and causes a diarrhoeal illness, cryptosporidiosis (Tzipori and Ward, 2002). Infections in immunocompetent individuals are normally asymptomatic or characterized by self-limiting diarrhoea, but it can develop into severe chronic, prolonged watery diarrhoea which is frequently fatal among immunocompromised patients, such as people with acquired immunodeficiency syndrome (Tzipori and Ward, 2002). As effective therapeutic or preventive interventions for cryptosporidiosis are not yet available, the development of effective anti-cryptosporidial drugs is urgently required. However, the poor experimental tractability of the protozoan parasite is one of the main obstacles to the development of effective vaccines or therapeutics.

Many protozoan parasites have been regarded as anaerobes, but these parasites have been recognized to be aerotolerant or microaerophilic, consuming oxygen to a certain extent (Mehlotra, 1996). Therefore, parasitic protozoa develop antioxidant systems to protect themselves from endogenous oxidative stress, as well as oxidative killing by host immune effector cells (Mehlotra, 1996; Nickel *et al.* 2006). Due to their essential roles in parasite physiology, antioxidant enzymes have been regarded as attractive drug targets for parasitic protozoa (Flohé *et al.* 1999; Andricopulo *et al.* 2006; Boucher *et al.* 2006; Nickel *et al.* 2006; Wilkinson *et al.* 2006; Na *et al.* 2007). The genome of *Cryptosporidium* also suggests that the parasite is capable of both aerobic and anaerobic metabolisms (Xu *et al.* 2004; Heiges *et al.* 2006), but it has been proposed that *Cryptosporidium* has a poor capacity to scavenge reactive oxygen species (ROS) compared with other protozoan parasites, which makes this parasite potentially more susceptible to ROS (Entrala *et al.* 1997). Indeed, ROS was observed to have protective roles in experimental *C. parvum* infection in the neonatal mouse (Leitch and He, 1999), which inversely suggests the essential role of an antioxidant system for the survival and pathology of the parasite. However, the antioxidant system of *C. parvum* is poorly understood and only a few enzymes, which are involved in the antioxidant defence mechanism, have been characterized in the parasite (Kang *et al.* 2008; Joung *et al.* 2011). Therefore, understanding the nature and mechanisms of the antioxidant system of

* Corresponding author: Department of Parasitology and Institute of Health Sciences, Gyeongsang National University School of Medicine, Jinju 660–751, Korea. E-mail: bkna@gnu.ac.kr

doi:10.1017/S0031182013001832

Cryptosporidium would be important to gain an insight into the biology of the parasite, as well as being important for the development of therapeutic drugs.

Glutathione peroxidase (GPx; EC 1.11.1.9) is one of the most important endogenous antioxidant enzymes and mediates antioxidant defence reactions by catalysing the reduction of organic hydroperoxides and hydrogen peroxide to water and oxygen using glutathione (GSH) as an electron donor (Herbette *et al*. 2007; Toppo *et al*. 2008). Global distribution of the enzyme in all oxygen-consuming organisms suggests a key protective role of the enzyme in cells/organisms from oxidative damage. The enzymes belonging to the GPx family share similar structural and enzymatic features with one another, and are classified into two large subfamilies of selenium-dependent GPx (Se-GPx) and selenium-independent GPx (NS-GPx). A cysteine residue encoded by UGU, which is located in the active site, is a specific feature of NS-GPxs, whereas Se-GPxs possess a seleno-cysteine (SeCys) residue encoded by UGA. The presence of a SeCys insertion sequence (SECIS) motif, a characteristic stem loop structure located downstream from the UGA codon which recognizes the UGA codon as a signal to insert a SeCys residue, in Se-GPxs is another important structural feature discriminating Se-GPxs from NS-GPxs (Herbette *et al*. 2007; Toppo *et al*. 2008).

The pivotal physiological roles of GPxs in parasitic protozoa have been acknowledged, and the enzymes have been postulated as potential chemotherapeutic drug targets (Wilkinson *et al*. 2000; Sztajer *et al*. 2001; Wilkinson and Kelly, 2003). In this study, we have identified a gene encoding GPx of *C. parvum* (CpGPx) and characterized biochemical properties of the recombinant enzyme.

MATERIALS AND METHODS

Identification and cloning of the gene encoding CpGPx

The gene encoding a CpGPx (Gene ID: cgd3_460) was identified by data-mining the *Cryptosporidium* Genomics Resources (CryptoDB, http://cryptodb.org). The open reading frame of CpGPx was amplified with forward (5′-ATGGGGAATTTTTTAGCATCCACAAAGATA-3′) and reverse (5′-TTAAGAACCTTGTTCACTTTGTTTTTTGCTT-3′) primers with Ex *Taq* DNA polymerase (Takara, Otsu, Japan) and *C. parvum* Iowa II genomic DNA. The amplified PCR product was gel-purified, ligated into the T&A cloning vector (Real Biotech Corporation, Banqiao City, Taiwan), and transformed into *Escherichia coli* DH5*α*. The nucleotide sequence of cloned gene was confirmed by automated DNA sequencing. Analysis of the primary structure of the deduced amino acid sequences was conducted with DNASTAR (DNASTAR, Madison, WI, USA), TMHMM (http://www.cbs.dtu.dk/services/TMHMM-2.0), and Signal P (http://www.cbs.dtu.dk/services/SignalP). TargetP1.1 (http://www.cbs.dtu.dk/services/TargetP) and PSORT (http://www.psort.org) were used to predict protein localization. SECISearch 2.19 (http://genome.unl.edu/SECISearch) was used for *in silico* detection of the SECIS motif within the 3′-untranslated region (UTR) of CpGPx.

Expression and purification of recombinant CpGPx

To express the recombinant CpGPx, the full-length gene of CpGPx was amplified using the primers 5′-GGATCCATGGGGAATTTTTTAGCATCCACA-3′, which contained a 5′ *Bam* HI site, and 5′-CTGCAGTTAAGAACCTTGTTCACTTTGTTTT-3′, which harboured a 5′ *Pst* I site. The PCR product was purified, ligated into the T&A cloning vector (Real Biotech Corporation), and transformed into *E. coli* DH5*α*. The resulting plasmid DNA was digested with the appropriate restriction enzymes and ligated into the pQE-30 expression vector (Qiagen, Valencia, CA, USA), which was then transformed into *E. coli* M15 [pREP4] cells (Qiagen). Selected clones were grown and induced with 1 mM isopropyl-1-thio-*β*-D-galactopyranoside (IPTG) at 37 °C for 3 h. The cells were harvested by centrifugation at 12 000 ***g*** for 15 min at 4 °C, and suspended in native lysis buffer (50 mM NaH_2PO_4, 300 mM NaCl, 10 mM imidazole, pH 8·0), sonicated on ice, and then centrifuged at 4 °C for 20 min at 12 000 ***g***. The recombinant CpGPx was purified by nickel-nitrilotriacetic acid (Ni-NTA) affinity chromatography (Qiagen), and the purification and purity of the recombinant protein was determined by sodium dodecyl sulphate-polyacrylamide gel electrophoresis (SDS-PAGE).

Enzyme assay

GPx activity was assayed by monitoring the glutathione reductase-catalysed nicotinamide adeninedinucleotide phosphate (NADPH; Sigma, St. Louis, MO, USA) oxidation at 37 °C in 200 *μ*L of assay buffer, which contained 0·3 mM NADPH, 0·1% Triton, 5 mM EDTA, 3 mM glutathione (GSH; Sigma), glutathione reductase (1·2 units mL^{-1}, Sigma), 73 mM cumene hydroperoxide (Cumene-OOH; Sigma) and 0·1 M Tris-HCl (pH 7·6). The level of NADPH oxidation was measured at 340 nm for 5 min by using Multiscan FC spectrophotometer (Thermo, Vantaa, Finland). All the reagents were prewarmed to room temperature before performance of the assay. As a negative control, bovine serum albumin (BSA, Sigma) was used in the reaction mixture. One unit of GPx activity was defined as the amount of enzyme required to cause the oxidation of 1 nM of NADPH per min under the above assay condition.

https://doi.org/10.1017/S0031182013001832 Published online by Cambridge University Press

Production of antibody for CpGPx (anti-CpGPx) and Western blot analysis

Specific antibody against recombinant CpGPx was produced by immunizing BALB/c mice with the purified recombinant protein (50 μg) three times at 2-week intervals. Two weeks after the final inoculation, the mice were euthanased and the sera were collected. The immunoglobulin G (IgG) fraction was isolated from the sera with a Protein G-Sepharose column (Amersham Biosciences, Piscataway, NJ, USA). The specificity of anti-CpGPx was determined by Western blot analysis. The oocysts of *C. parvum* (Iowa strain) passaged in calves were purchased from Waterborne Inc. (P102C; New Orleans, LA, USA). The oocysts (10^7) were excysted by incubation in excystation medium (0·5% trypsin, pH 2·5) for 30 min at 37 °C. The excysted sporozoites were immediately collected, rinsed five times with sterile phosphate buffered saline (PBS; pH 7·4), and suspended in sterile PBS which contained complete protease inhibitor cocktail (Roche, Mannheim, Germany). The excysted sporozoites were confirmed by examination under microscopy. The sporozoites were sonicated on ice using 5-s pulses at 50% output power for up to 3 min in a W-380/385-series SONICATOR Ultrasonic Liquid Processor (Misonix Inc., Farmingdale, NY, USA). The soluble extract of *C. parvum* sporozoites (20 μg) was collected by centrifugation and subjected to SDS–PAGE, and the proteins were transferred to a nitrocellulose membrane (Bio-Rad, Hercules, CA, USA). The membrane was blocked with PBS supplemented with 0·05% Tween 20 (PBST, pH 7·4) and 3% skim milk for 1 h. The membrane was then incubated with anti-CpGPx which was diluted 1:1000 in PBST at room temperature for 2 h. After several washes with PBST, the membrane was incubated with 1:1000 diluted horseradish peroxidase-conjugated goat anti-mouse IgG (Sigma). The blot was visualized with 4-chloro-1-naphthol (Sigma) and the reaction was stopped by washing the membrane with distilled water.

Biochemical properties of recombinant CpGPx

The optimal pH for the maximum activity of CpGPx was assessed in sodium acetate (pH 5·0–5·5), sodium phosphate (pH 6·0–6·5), Tris-HCl (pH 7·0–8·5) and glycine–NaOH (pH 9·0). Recombinant CpGPx was added to each pH buffer supplemented with all chemicals and enzymes and the enzyme activity was measured as described above. For each pH, the appropriate blank was separately measured as a control. The pH stability of CpGPx was also examined at pH 5·0, 6·0, 7·0, 8·0 or 9·0 by incubating the enzyme at 37 °C in the appropriate buffers. Substrate specificity of CpGPx was determined its relative activity against different hydroperoxide substrates, cumene-OOH, *t*-butyl hydroperoxide (*t*-butyl-OOH) or hydrogen peroxide (H_2O_2). For inhibitor test, CpGPx was preincubated with different concentrations (0·01 to 10 mM) of potassium cyanide (KCN) or sodium azide (NaN_3) in 50 mM Tris–HCl (pH 7·5) at room temperature for 1 h. The residual enzyme activity of each sample was measured using cumene-OOH as a substrate. All assays were carried out triplicate and the mean and standard deviation (S.D.) were calculated.

Fast protein liquid chromatography (FPLC)

To determine the molecular structure of CpGPx, gel filtration chromatography was performed with a Superdex 200 HR 10/30 column using an Äcta FPLC system (GE Biosciences, Pittsburgh, PA, USA). The column was equilibrated and eluted with 20 mM Tris–HCl (pH 8·0) containing 0·15 M NaCl at a flow rate of 0·5 mL min^{-1}. Recombinant CpGPx was loaded onto the column, and fractions (each 0·5 mL) were collected. The collected fractions were analysed by both enzyme assay and SDS-PAGE analysis. The column was calibrated with the following molecular weight markers (Sigma): blue dextran (*M*r 2000 kDa), β-amylase (*M*r 200 kDa), alcohol dehydrogenase (*M*r 150 kDa), BSA (*M*r 66 kDa), carbonic anhydrase (*M*r 29 kDa) and cytochrome c (*M*r 12·4 kDa). The K_{av} value for each protein was calculated according to the equation: $K_{av} = (V_e - V_0)/(V_t - V_0)$, where V_e is the elution volume of the protein, V_0 is the elution volume of blue dextran and V_t is the total bed volume.

Protective role of CpGPx from oxidative damage

The protective role of CpGPx on DNA and protein from oxidative damage was analysed. pET-45b plasmid (Novagen; La Jolla, CA, USA) was incubated with different concentrations (0, 0·1 and 0·2%) of H_2O_2 in the presence or absence of different amounts of recombinant CpGPx at 37 °C for 2 h and was analysed by agarose gel electrophoresis. For the protein assay, BSA (10 μg) was incubated with different concentrations (0, 0·1 and 0·2%) of H_2O_2 in the presence or absence of different amounts of recombinant CpGPx at 37 °C for 2 h, and was then analysed by SDS-PAGE.

Expression profile of CpGPx

The expression pattern of CpGPx in different developmental stages of *C. parvum* was analysed by *in vitro* cultivation followed by semi-quantitative reverse transcription PCR (RT–PCR). For *in vitro* cultivation assay, the oocysts of *C. parvum* (10^7) were bleached with 1:20 diluted household bleach for 30 min at room temperature to sterilize the parasites,

https://doi.org/10.1017/S0031182013001832 Published online by Cambridge University Press

and were then washed three times with sterile phosphate buffered saline (PBS, pH 7·4) as described previously (Borowski *et al*. 2010). Sterilized oocysts were incubated in 0·2 μm membrane-filtered excystation medium (0·5% trypsin, pH 2·5) for 30 min at 37 °C. The excysted sporozoites were collected, rinsed five times with sterile PBS, and then were suspended in serum-free RPMI medium. The excysted sporozoites were confirmed by microscopic examination. The sporozoites of *C. parvum* were experimentally infected to human ileocaecal epithelial cells (HCT-8, ATCC CCL-244; American Type Culture Collection, Rockville, MD, USA) by adding 10^5 sporozoites to HCT-8 cells which were grown to a 70% confluent monolayer in 6-well plates, and the cells were then incubated at 37 °C with 5% CO_2 for 1 h. The supernatant was discarded and the cells were washed with PBS several times to remove any uninfected *C. parvum* sporozoites. After adding fresh RPMI medium with 10% fetal bovine serum to each well, the cells were incubated at 37 °C in 5% CO_2 for 6, 12, 24, 36, 48 and 60 h, respectively. The cells were collected at each indicated time point and infection was quantified by an enzyme-linked immunosorbent assay, as described previously (Wanyiri *et al*. 2007). Total RNAs were isolated from each sample using Trizol reagent (Invitrogen, Carlsbad, CA, USA) and semi-quantitative RT–PCR was performed with equal amounts of total RNA (1 μg each) and CpGPx specific primers. The RNAs purified from excysted sporozoites were also included. PCR products were analysed on 1·5% agarose gel with ethidium bromide staining. *Cryptosporidium parvum* heat shock protein 70 (CpHSP70; cdg2_20), which is reported to be constitutively expressed in different developmental stages of *C. parvum* (Shahiduzzaman *et al*. 2009), was included as a standard control. The COWP6 (cdg4_3090), a major oocyst wall protein expressed in oocyst of *C. parvum* (Chatterjee *et al*. 2010), and enolase (cdg5_1960), the expression of which is spiked in immature meronts (Mauzy *et al*. 2012), were also analysed to verify the development of the parasite.

RESULTS

Molecular characterization of CpGPx

The gene encoding CpGPx consisted of 657 bp that encoded 218 amino acid residues with a predicted molecular mass of 24·8 kDa. The deduced amino acid sequence alignment of CpGPx and several GPxs from other organisms is shown in Fig. 1. CpGPx showed 11·5–26·3% sequence identity to those from the GPx superfamily of human, and was more related to GPx4 (phospholipid hydroperoxide GPx; PHGPx) than to any of the other GPx types. CpGPx showed higher sequence identity to GPxs from plants and yeast than those of mammals. Neither potential signal peptide sequence nor putative glycosylation site was found in the sequence of CpGPx. The three amino acid residues, Cys^{51}, Gln^{86} and Trp^{145}, which form the catalytic triad of GPxs (Toppo *et al*. 2008), were well conserved in CpGPx. As plant GPx-like proteins, CpGPx contained the standard codon for cysteine (UGU), rather than the opal UGA codon for SeCys at the catalytic site (Fig. 1). *In silico* prediction analysis of the SECIS motif within the 3′-UTR of CpGPx revealed that no SECIS motif was found in the sequence (data not shown), which suggested its selenium-independent nature. Prediction analysis for cellular localization of CpGPx implied that this enzyme is most likely to be localized in cytosol (data not shown). The PGGG motif and oligomerization interface, which are associated with a tetrameric structure formation and are well-conserved in tetrameric GPxs (Toppo *et al*. 2008), were not identified in CpGPx. However, GPxs of *Cryptosoporidium* and *Plasmodium* species had a short insert, consisting of 14–15 amino acids, in the corresponding region of the oligomerization interface in mammalian tetrameric GPxs. Phylogenetic analysis revealed that CpGPx was closely related to GPxs of other sporozoan parasites, including *Cryptosporidium* spp., *Plasmodium* spp., *Toxoplasma gondii* and *Perkinsus marinus* (Fig. 2).

Expression and biochemical properties of CpGPx

Recombinant CpGPx was successfully expressed in *E. coli* as a soluble protein of about 25 kDa, which coincided with an estimated molecular mass (Fig. 3A). To confirm the expression of CpGPx in *C. parvum*, we performed Western blot analysis using anti-CpGPx and a soluble extract of *C. parvum* sporozoites. Anti-CpGPx was specifically reacted with a protein band having an approximate molecular mass of 25 kDa, which coincided well with the size of recombinant CpGPx, suggesting that CpGPx is functionally expressed in *C. parvum* sporozoites (Fig. 3B). CpGPx was proven to be monomeric when subjected to Superdex 200 HR 10/30 gel filtration under non-reducing condition. It eluted in the fractions corresponding to the approximate molecular mass of 25 kDa, whereas no activity could be detected in the fractions corresponding to the molecular mass of dimeric or tetrameric forms (data not shown). Recombinant CpGPx was active over a wide pH range with a maximum activity at pH 7·5 (Fig. 4A) and was stable under physiological conditions. The recombinant enzyme showed the activity of $84{\cdot}3 \pm 5{\cdot}8$ units mg^{-1} protein for cumene-OOH. It showed substrate preference against organic hydroperoxides, such as cumene-OOH and *t*-butyl-OOH, but it showed low activity against inorganic hydroperoxide, H_2O_2 (Fig. 4B). The activity of

https://doi.org/10.1017/S0031182013001832 Published online by Cambridge University Press

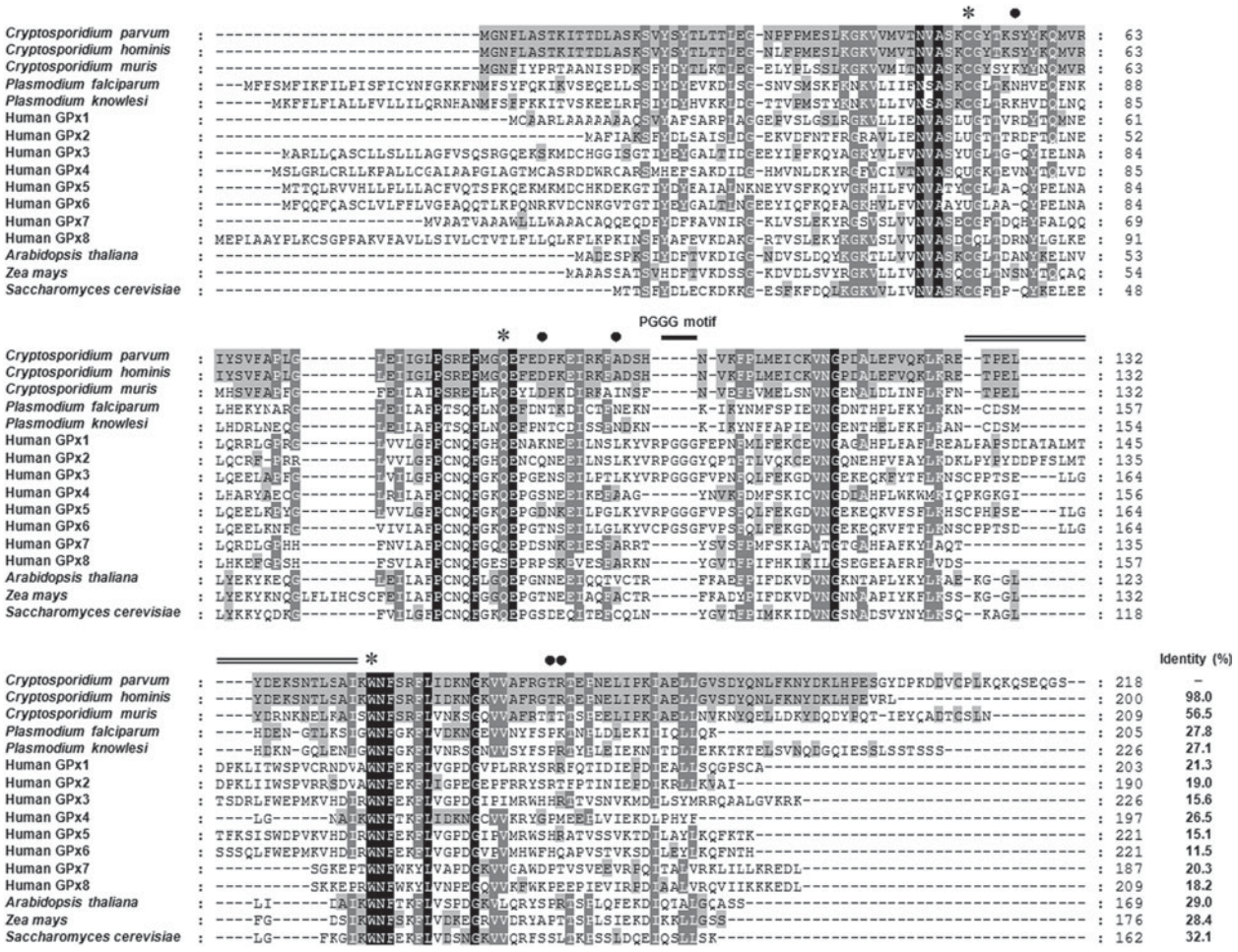

Fig. 1. Multiple sequence alignment analysis. The deduced amino acid sequence of CpGPx was aligned with those of GPxs from *Cryptosporidium hominis* (XP_668297), *Cryptosporidium muris* (XP_002139111), *Plasmodium falciparum* (XP_001350528), *Plasmodium knowlesi* (XP_002260396), Human GPx1 (NP_000572), Human GPx2 (NP_002074), Human GPx3 (NP_002075), Human GPx4 (NM_002085), Human GPx5 (NP_001500), Human GPx6 (NP_874360), Human GPx7 (NP_056511), Human GPx8 (NP_001008398), *Arabidopsis thaliana* (AJ000470), *Zea mays* (AA582602), and *Saccharomyces cerevisiae* (P38143). Gaps are introduced into the sequences to maximize alignment. The asterisks indicate the catalytic triad (Cys, Gln and Trp). The amino acid residues involved in binding of the GSH molecule are marked with closed circles. The PGGG motif and oligomerization interface are indicated by bold line and double line on the sequence, respectively. The shading represents the degree of identity among the sequences: black (100%), dark grey (50–92%) and light grey (15–49%). Sequence identity of CpGPx to other GPxs is represented on the right. The abbreviation 'U' represents seleno-cysteine (SeCys).

CpGPx was not inhibited by either KCN or NaN_3 (Fig. 4C). CpGPx was not inhibited by KCN, even though the enzyme was preincubated with high concentration of KCN (20 mM) for up to 3 h (data not shown).

Protective role of CpGPx from oxidative damage

To analyse the protective role of CpGPx towards oxidative damage of biomolecules, we assayed the protection activity of CpGPx on DNA and protein from oxidative damage induced by H_2O_2. Recombinant CpGPx effectively protected plasmid DNA from H_2O_2-induced oxidative damage in a dose-dependent manner (Fig. 5A). The H_2O_2-untreated plasmid DNA showed a major single band corresponding to the supercoiled form (S form). Treatment with H_2O_2 resulted in oxidative damage of plasmid DNA, which was evaluated by assessing the shift in the mobility of plasmid DNA, which resulted from cleavage into a nicked circular form (N form), in proportion to H_2O_2 concentration. Treatment of CpGPx inhibited the conversion of the S form into the N form of plasmid DNA in the presence of H_2O_2 in a dose-dependent pattern, which indicated that CpGPx protected plasmid DNA against oxidative damage. Incubation of BSA with H_2O_2 also induced oxidative damage of the protein, which resulted in degradation of BSA into various sizes of smaller fragments (Fig. 5B). Treatment of CpGPx also effectively inhibited H_2O_2-induced damage of BSA in a dose-dependent manner.

https://doi.org/10.1017/S0031182013001832 Published online by Cambridge University Press

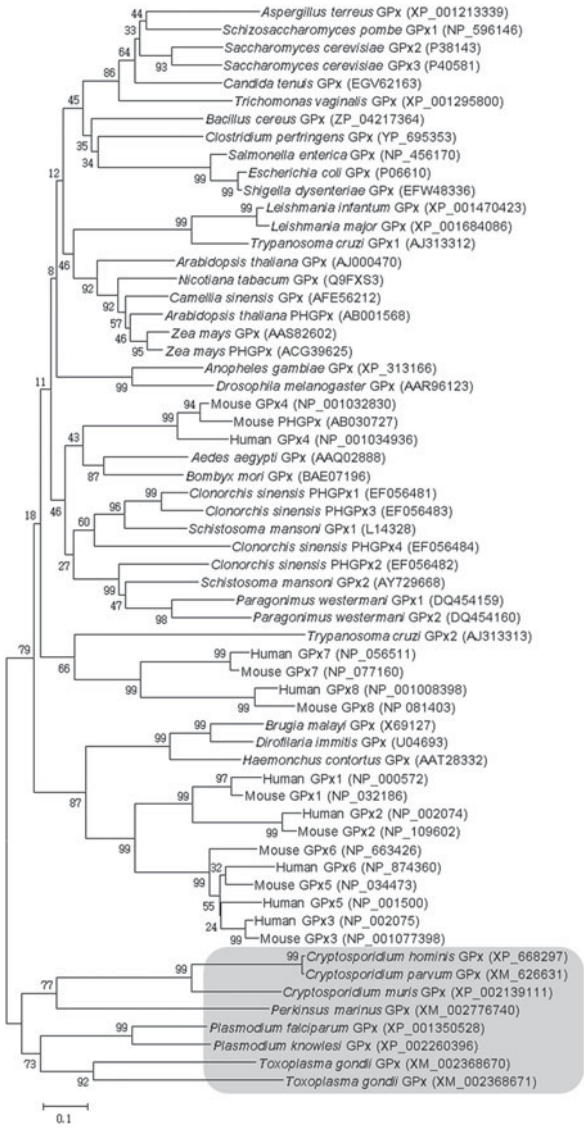

Fig. 2. Phylogenetic analysis. The phylogenetic tree was constructed with the neighbour-joining method using the MEGA4 program. Numbers on the branches indicate bootstrap proportions (1000 replicates).

Expression profile of CpGPx in different developmental stages of C. parvum

To analyse the expression pattern of CpGPx in different developmental stages of *C. parvum*, we performed *in vitro* cultivation of the parasite using HCT-8 cells as host cells followed by semi-quantitative RT-PCR analysis using total RNA collected at different time points after infection. The amplification of CpGPx transcripts demonstrated that the gene was transcribed throughout all of the developmental stages of the parasite examined in this study (Fig. 6). To validate the development of the parasite in the cultivation system, we also performed semi-quantitative RT-PCR analysis for three *C. parvum* genes, including HSP70, enolase and COWP6, the expression patterns of which have been previously demonstrated (Shahiduzzaman *et al.* 2009; Chatterjee *et al.* 2010; Mauzy *et al.* 2012). All tested control genes were confirmed to be expressed at corresponding developmental stages.

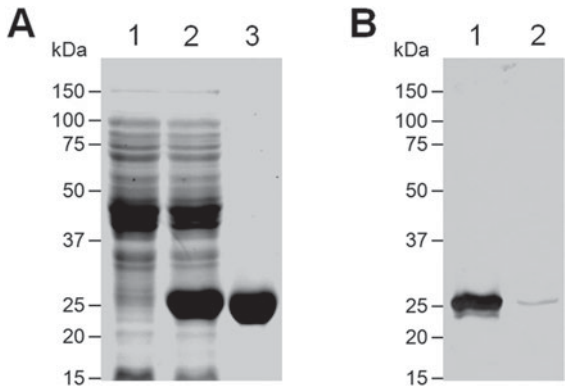

Fig. 3. Expression and purification of recombinant CpGPx. (A) Expression and purification. A full-length gene of CpGPx was ligated into pQE-30 expression vector and transformed into *E. coli* M15 [pREP4] cells. Expression of recombinant protein was induced with 1 mM IPTG. Proteins were analysed by SDS–PAGE and stained with Coomassie blue. Lane 1, *E. coli* lysate control; lane 2, IPTG-induced *E. coli* lysate; lane 3, recombinant CpGPx purified with Ni-NTA affinity chromatography; (B) Western blot analysis. Recombinant CpGPx and the soluble extract of *C. parvum* sporozoites were separated on SDS-PAGE and the proteins were transferred to nitrocellulose membrane. The blot was probed with anti-CpGPx. Lane 1, recombinant CpGPx (5 μg); lane 2, soluble extract of *C. parvum* sporozoites (20 μg).

DISCUSSION

Sequence analysis of CpGPx suggested that the enzyme is a member of cytosolic NS-GPx family. Immunoblot analysis using soluble extract of *C. parvum* sporozoites and anti-CpGPx antibody also suggests that the enzyme is a cytosolic protein which is functionally expressed in sporozoites of the parasite. Protozoan GPxs have been acknowledged to be classified into two subclades which cluster in the same branches of the monomeric forms of the human GPx family, including GPx-4, GPx-7 and GPx-8 (Toppo *et al.* 2008). CpGPx also showed higher sequence identity with monomeric GPxs than with tetrameric GPxs of mammals. Absences of the PGGG motif and oligomerization interface, which are involved in the formation of tetrameric structures (Toppo *et al.* 2008), in CpGPx also imply that the enzyme has a monomeric structure. Both PAGE analysis under non-reducing conditions and gel filtration analysis of recombinant CpGPx also support the notion that CpGPx is a monomeric protein. Sequence and phylogenetic analyses of CpGPx also revealed that CpGPx showed higher sequence identity with plant and yeast GPxs than with animal GPxs. However, this is not surprising given that close

https://doi.org/10.1017/S0031182013001832 Published online by Cambridge University Press

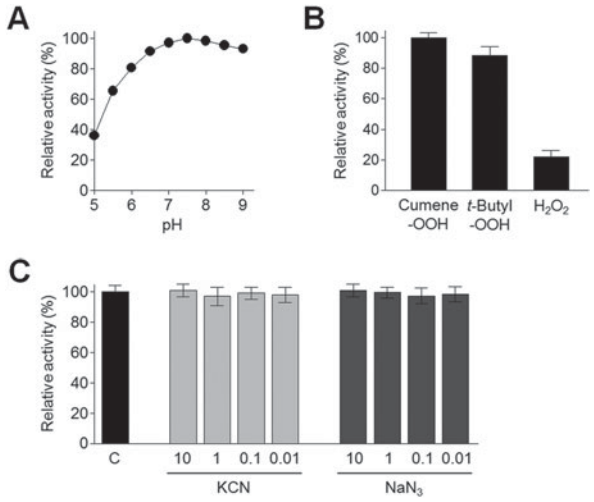

Fig. 4. Biochemical properties of CpGPx. (A) Optimal pH. Enzyme activity was assayed in different pH buffers ranging from pH 5·0–9·0 by using cumene-OOH as a substrate. For each pH, the appropriate blank was separately measured as the control group. Maximal activity was represented as 100%. Three independent assays for each pH were carried out and the mean value was calculated. (B) Substrate specificity. Enzyme activity of CpGPx for different hydroperoxide substrates, cumene-OOH, *t*-butyl-OOH or H_2O_2, was assayed. Maximal activity observed for cumene-OOH was represented as 100%. All the assays were carried out triplicate and the mean and standard deviation (S.D.) were calculated. (C) Inhibition assay. CpGPx was preincubated with different concentrations of KCN or NaN_3 in 50 mM Tris-HCl (pH 7·5) at room temperature for 20 min. The residual enzyme activity of each sample was measured using cumene-OOH as a substrate. C, control CpGPx without pretreatment of any chemical. All the assays were carried out triplicate and the mean and standard deviation (S.D.) were calculated.

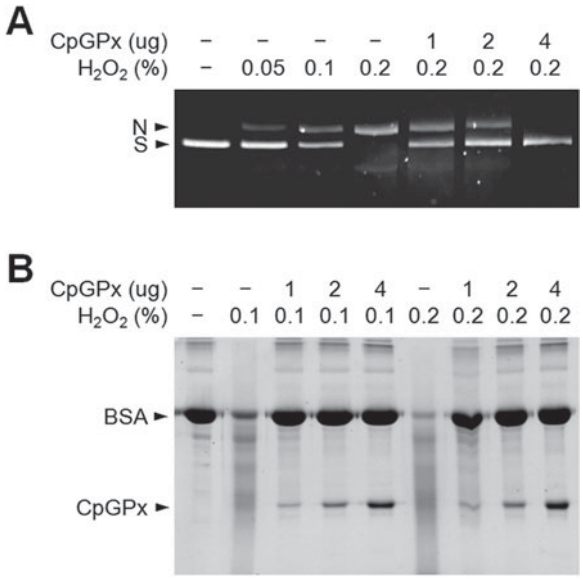

Fig. 5. Protection of DNA and protein from oxidative damage by CpGPx. (A) DNA cleavage assay. pET-45b plasmid was incubated with different concentrations of H_2O_2 in the presence or absence of different concentrations of recombinant CpGPx at 37 °C for 2 h and was analysed by agarose gel electrophoresis. N, nicked plasmid; S, supercoiled plasmid; (B) Protein damage assay. BSA (10 μg) was incubated with different concentrations of H_2O_2 in the presence or absence of different concentrations of recombinant CpGPx at 37 °C for 2 h and analysed by SDS–PAGE.

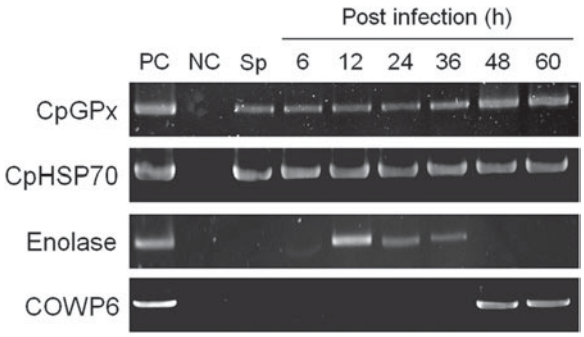

Fig. 6. Expression profile of CpGPx in the developmental stages of *C. parvum*. The sporozoites of *C. parvum* were experimentally infected to HCT-8 cells and the cells were collected at each indicated time point after infection. Total RNAs were isolated from each sample and semi-quantitative RT–PCR was performed with equal amounts of total RNA (1 μg each) and specific primers. PCR products were analysed on a 1·5% agarose gel with ethidium bromide staining. CpHSP70, *C. parvum* heat shock protein 70 (cdg2_20); enolase, *C. parvum* enolase (cdg5_1960); COWP6, *C. parvum* oocyst wall protein 6 (cdg4_3090); PC, positive control (cloned gene); NC, control HCT-8 cells without infection with *C. parvum* sporozoites; Sp, sporozoites.

association and common ancestry of apicomplexa protozoa parasites with plants, cyanobacteria, and algae have been previously suggested (Wilson *et al.* 1994; Stack *et al.* 2007; Yu *et al.* 2010; Kang *et al.* 2011).

Biochemical properties of CpGPx also propose that this enzyme is a member of the NS-GPx family of enzymes. One of the major functional differences between Se-GPxs and NS-GPxs is that Se-GPxs catalyse the reduction of both organic and inorganic peroxides like H_2O_2, whereas NS-GPxs react preferentially with organic peroxides (Tang *et al.* 1995; Sun *et al.* 2012). CpGPx showed a substrate preference against organic hydroperoxide, such as cumene-OOH and *t*-butyl-OOH, rather than inorganic hydroperoxide, H_2O_2, which is coincided with previous results from NS-GPx family enzymes of other organisms (Tang *et al.* 1995; Wilkinson *et al.* 2000; Jones *et al.* 2004; Sun *et al.* 2012). KCN is known to inhibit Se-GPxs by inducing the release of selenium, which is essential for Se-GPxs to maintain their activities, from the active site of the enzymes (Prohaska *et al.* 1977; Awasthi *et al.* 1979; Singh and Rathaur, 2005). However, CpGPx activity was not affected by KCN even though the enzyme was pretreated with a high concentration of KCN (20 mM) up

https://doi.org/10.1017/S0031182013001832 Published online by Cambridge University Press

to 3 h, which indicated that CpGPx does not have selenium in its active site. NaN_3, an inhibitor of heme proteins, also did not affect CpGPx activity.

Some NS-GPxs, including GPxs of *Plasmodium falciparum* and *Trypanosoma brucei*, show a high affinity for thioredoxin to reduce organic hydroperoxides (Wilkinson *et al*. 2000; Sztajer *et al*. 2001; Herbette *et al*. 2002; Maiorino *et al*. 2007). This leads them to be classified into a novel functional class of thioredoxin GPx-like peroxidase (TGPx) based on the prominent preference for thioredoxin as an electron donor (Toppo *et al*. 2008). Most cytosolic GPxs showed pronounced specificity against GSH (Flohé *et al*. 1971) and this specificity is considered to be due to basic amino acid residues, Arg^{57}, Lys^{92}, Arg^{102}, Arg^{184} and Arg^{185}, which direct the SH group of the substrate to the active-site selenium atom by electrostatic forces (Aumann *et al*. 1997). However, these residues are only partially conserved in CpGPx and the enzyme does not contain SeCys at its active site, and therefore, it would be interesting to analyse further whether CpGPx has thioredoxin peroxidase activity.

The expression of CpGPx in all tested developmental stages of *C. parvum* suggests its essential role in the physiology of the parasite. In organisms which have both Se-GPxs and NS-GPxs, it has been postulated that Se-GPxs are the main enzymes for scavenging H_2O_2 and preventing the further formation of ROS, but NS-GPxs contribute only an adequate function as a backup system for Se-GPxs in the absence of sufficient concentrations of selenium (Vernet *et al*. 1999). This postulation is mainly due to the less efficient ROS-detoxifying activity of NS-GPxs than Se-GPxs. Unlike other apicomplexa protozoan parasites, such as *Plasmodium* species and *T. gondii*, *Cryptosporidium* species are not likely to utilize SeCys since neither selenoproteins nor SeCys insertion systems have been found in genomes of the parasite (Lobanov *et al*. 2006). Considering the high sequence homology of NS-GPxs with the mammalian membrane-bound GPx4 (PHGPx), most NS-GPxs have been proposed to be involved in reducing membrane peroxidation (Herbette *et al*. 2007). Several studies have provided experimental evidence that NS-GPxs efficiently reduce lipid peroxides as well as a broad range of peroxide *in vitro* (Gaber *et al*. 2001; Herbette *et al*. 2002; Jung *et al*. 2002). Our data clearly demonstrated that CpGPx effectively protect DNA and protein from H_2O_2-induced oxidative damage. H_2O_2 is an uncharged molecule and can freely diffuse across biological membranes and is able to access any sub-cellular compartment within cells. Inside the cells, it can induce damage of diverse cellular macromolecules such as nucleic acids, proteins and lipids directly, or indirectly following the generation of hydroxyl radicals (Ohno and Gallin, 1985). CpGPx may play a critical role in the protection of biomolecules of *C. parvum* against endogenous and/or exogenous H_2O_2. However, considering that CpGPx showed weak activity against H_2O_2 compared with short chain organic hydroperoxides, it is possible that this enzyme could also participate in detoxifying secondary oxidation products which are generated during lipid peroxidation reactions. However, it is not currently clear whether CpGPx shows activity for phospholipid hydroperoxides, and this should be further elucidated. It has been previously reported that *C. parvum* does not have catalase and GPx activities (Entrala *et al*. 1997). We also confirmed that *C. parvum* lacks catalase in its genome from a data search of CryptoDB, but our results clearly demonstrate that *C. parvum* has a functional GPx. Currently, only a few antioxidant enzymes, including iron-superoxide dismutase and TPx, have been characterized in the parasite (Kang *et al*. 2008; Joung *et al*. 2011). And therefore, identification for other candidates that exert antioxidant defence in *C. parvum* and characterization of biochemical and functional properties of the candidates would allow further insight into the understanding of the antioxidant defence mechanism of the parasite.

FINANCIAL SUPPORT

This research was supported by the Basic Science Research Programme through the National Research Foundation of Korea (NRF) funded by the Ministry of Education, Science and Technology (NRF-2010-0021687).

REFERENCES

Andricopulo, A. D., Akoachere, M. B., Krogh, R., Nickel, C., McLeish, M. J., Kenyon, G. L., Arscott, L. D., Williams, C. H., Jr., Davioud-Charvet, E. and Becker, K. (2006). Specific inhibitors of *Plasmodium falciparum* thioredoxin reductase as potential antimalarial agents. *Bioorganic and Medicinal Chemistry Letters* **16**, 2283–2292.

Aumann, K.-D., Bedorf, N., Brigelius-Flohé, R., Schomburg, D. and Flohé, L. (1997). Glutathione peroxidase revisited – simulation of the catalytic cycle by computer-assisted molecular modelling. *Biomedical and Environmental Sciences* **10**, 136–155.

Awasthi, Y. C., Dao, D. D., Lal, A. K. and Srivastava, S. K. (1979). Purification and properties of glutathione peroxidase from human placenta. *Biochemical Journal* **177**, 471–476.

Borowski, H., Thompson, R. C., Armstrong, T. and Clode, P. L. (2010). Morphological characterization of *Cryptosporidium parvum* life-cycle stages in an *in vitro* model system. *Parasitology* **137**, 13–26.

Boucher, I. W., Brzozowski, A. M., Brannigan, J. A., Schnick, C., Smith, D. J., Kyes, S. A. and Wilkinson, A. J. (2006). The crystal structure of superoxide dismutase from *Plasmodium falciparum*. *BMC Structural Biology* **6**, 20.

Chatterjee, A., Banerjee, S., Steffen, M., O'Connor, R. M., Ward, H. D., Robbins, P. W. and Samuelson, J. (2010). Evidence for mucin-like glycoproteins that tether sporozoites of *Cryptosporidium parvum* to the inner surface of the oocyst wall. *Eukaryotic Cell* **9**, 84–96.

Entrala, E., Mascaro, C. and Barrett, J. (1997). Anti-oxidant enzymes in *Cryptosporidium parvum* oocysts. *Parasitology* **114**, 13–17.

Flohé, L., Günzler, W. A., Jung, G., Schaich, E. and Schneider, F. (1971). Glutathione peroxidase. II. Substrate specificity and inhibitory effects of substrate analogues. *Hoppe-Seyler's Zeitschrift für Physiologische Chemie* **352**, 159–169.

Flohé, L., Hecht, H. J. and Steinert, P. (1999). Glutathione and trypanothione in parasitic hydroperoxide metabolism. *Free Radical Biology and Medicine* **27**, 966–984.

Gaber, A., Tamoi, M., Takeda, T., Nakano, Y. and Shigeoka, S. (2001). NADPH-dependent glutathione peroxidase-like proteins (Gpx-1, Gpx-2)

https://doi.org/10.1017/S0031182013001832 Published online by Cambridge University Press

reduce unsaturated fatty acid hydroperoxides in Synechocystis PCC 6803. *FEBS Letters* **499**, 32–36.

Heiges, M., Wang, H., Robinson, E., Aurrecoechea, C., Gao, X., Kaluskar, N., Rhodes, P., Wang, S., He, C. Z., Su, Y., Miller, J., Kraemer, E. and Kissinger, J. C. (2006). CryptoDB: a *Cryptosporidium* bioinformatics resource update. *Nucleic Acids Research* **34**, D419–D422.

Herbette, S., Lenne, C., Leblanc, N., Julien, J. L., Drevet, J. R. and Roeckel-Drevet, P. (2002). Two GPX-like proteins from *Lycopersicon esculentum* and *Helianthus annuus* are antioxidant enzymes with phospholipid hydroperoxide glutathione peroxidase and thioredoxin peroxidase activities. *European Journal of Biochemistry* **269**, 2414–2420.

Herbette, S., Roeckel-Drevet, P. and Drevet, J. R. (2007). Seleno-independent glutathione peroxidases. More than simple antioxidant scavengers. *FEBS Journal* **274**, 2163–2180.

Jones, J. T., Reavy, B., Smant, G. and Prior, A. E. (2004). Glutathione peroxidases of the potato cyst nematode *Globodera rostochiensis*. *Gene* **324**, 47–54.

Joung, M., Yoon, S., Choi, K., Kim, J. Y., Park, W. Y. and Yu, J. R. (2011). Characterization of the thioredoxin peroxidase from *Cryptosporidium parvum*. *Experimental Parasitology* **129**, 331–336.

Jung, B. G., Lee, K. O., Lee, S. S., Chi, Y. H., Jang, H. H., Kang, S. S., Lee, K., Lim, D., Yoon, S. C., Yun, D. J., Inoue, Y., Cho, M. J. and Lee, S. Y. (2002). A chinese cabbage cDNA with high sequence identity to phospholipid hydroperoxide glutathione peroxidases encodes a novel isoform of thioredoxin-dependent peroxidase. *Journal of Biological Chemistry* **277**, 12572–12578.

Kang, J. M., Cheun, H. I., Kim, J., Moon, S. U., Park, S. J., Kim, T. S., Sohn, W. M. and Na, B. K. (2008). Identification and characterization of a mitochondrial iron-superoxide dismutase of *Cryptosporidium parvum*. *Parasitology Research* **103**, 787–795.

Kang, J. M., Ju, H. L., Sohn, W. M. and Na, B. K. (2011). Molecular cloning and characterization of a M17 leucine aminopeptidase of *Cryptosporidium parvum*. *Parasitology* **18**, 1–9.

Leitch, G. J. and He, Q. (1999). Reactive nitrogen and oxygen species ameliorate experimental cryptosporidiosis in the neonatal BALB/c mouse model. *Infection and Immunity* **67**, 5885–5891.

Lobanov, A. V., Delgado, C., Rahlfs, S., Novoselov, S. V., Kryukov, G. V., Gromer, S., Hatfield, D. L., Becker, K. and Gladyshev, V. N. (2006). The *Plasmodium* selenoproteome. *Nucleic Acids Research* **34**, 496–505.

Maiorino, M., Ursini, F., Bosello, V., Toppo, S., Tosatto, S. C., Mauri, P., Becker, K., Roveri, A., Bulato, C., Benazzi, L., De Palma, A. and Flohé, L. (2007). The thioredoxin specificity of *Drosophila* GPx: a paradigm for a peroxiredoxin-like mechanism of many glutathione peroxidases. *Journal of Molecular Biology* **365**, 1033–1046.

Mauzy, M. J., Enomoto, S., Lancto, C. A., Abrahamsen, M. S. and Rutherford, M. S. (2012). The *Cryptosporidium parvum* transcriptome during *in vitro* development. *PLoS ONE* **7**, e31715.

Mehlotra, R. K. (1996). Antioxidant defense mechanisms in parasitic protozoa. *Critical Reviews in Microbiology* **22**, 295–314.

Na, B. K., Kang, J. M., Kim, T. S. and Sohn, W. M. (2007). *Plasmodium vivax*: molecular cloning, expression and characterization of glutathione S-transferase. *Experimental Parasitology* **116**, 414–418.

Nickel, C., Rahlfs, S., Deponte, M., Koncarevic, S. and Becker, K. (2006). Thioredoxin networks in the malarial parasite *Plasmodium falciparum*. *Antioxidants and Redox Signaling* **8**, 1227–1239.

Ohno, Y. and Gallin, J. I. (1985). Diffusion of extracellular hydrogen peroxide into intracellular compartments of human neutrophils. Studies utilizing the inactivation of myeloperoxidase by hydrogen peroxide and azide. *Journal of Biological Chemistry* **260**, 843–846.

Prohaska, J. R., Oh, S. H., Hoekstra, W. G. and Ganther, H. E. (1977). Glutathione peroxidase: inhibition by cyanide and release of selenium. *Biochemical and Biophysical Research Communications* **74**, 69–71.

Shahiduzzaman, M., Dyachenko, V., Obwaller, A., Unglaube, S. and Daugschies, A. (2009). Combination of cell culture and quantitative PCR for screening of drugs against *Cryptosporidium parvum*. *Veterinary Parasitology* **162**, 271–277.

Singh, A. and Rathaur, S. (2005). Identification and characterization of a selenium-dependent glutathione peroxidase in *Setaria cervi*. *Biochemical and Biophysical Research Communications* **331**, 1069–1074.

Stack, C. M., Lowther, J., Cunningham, E., Donnelly, S., Gardiner, D. L., Trenholme, K. R., Skinner-Adams, T. S., Teuscher, F., Grembecka, J., Mucha, A., Kafarski, P., Lua, L., Bell, A. and Dalton, J. P. (2007). Characterization of the *Plasmodium falciparum* M17 leucyl aminopeptidase. A protease involved in amino acid regulation with potential for antimalarial drug development. *Journal of Biological Chemistry* **282**, 2069–2080.

Sun, W., Song, X., Yan, R., Xu, L. and Li, X. (2012). Cloning and characterization of a selenium-independent glutathione peroxidase (HC29) from adult *Haemonchus contortus*. *Journal of Veterinary Science* **13**, 49–58.

Sztajer, H., Gamain, B., Aumann, K. D., Slomianny, C., Becker, K., Brigelius-Flohé, R. and Flohé, L. (2001). The putative glutathione peroxidase gene of *Plasmodium falciparum* codes for a thioredoxin peroxidase. *Journal of Biological Chemistry* **276**, 7397–7403.

Tang, L., Gounaris, K., Griffiths, C. and Selkirk, M. E. (1995). Heterologous expression and enzymatic properties of a selenium-independent glutathione peroxidase from the parasitic nematode *Brugia pahangi*. *Journal of Biological Chemistry* **270**, 18313–18318.

Toppo, S., Vanin, S., Bosello, V. and Tosatto, S. C. (2008). Evolutionary and structural insights into the multifaceted glutathione peroxidase (Gpx) superfamily. *Antioxidants and Redox Signaling* **10**, 1501–1514.

Tzipori, S. and Ward, H. (2002). Cryptosporidosis: biology, pathogenesis and disease. *Microbes and Infection* **4**, 1047–1058.

Vernet, P., Rock, E., Mazur, A., Rayssiguier, Y., Dufaure, J. P. and Drevet, J. R. (1999). Selenium-independent epididymis-restricted glutathione peroxidase 5 protein (GPX5) can back up failing Se-dependent GPXs in mice subjected to selenium deficiency. *Molecular Reproduction and Development* **54**, 362–370.

Wanyiri, J. W., O'Connor, R., Allison, G., Kim, K., Kane, A., Qiu, J., Plaut, A. G. and Ward, H. D. (2007). Proteolytic processing of the *Cryptosporidium* glycoprotein gp40/15 by human furin and by a parasite-derived furin-like protease activity. *Infection and Immunity* **75**, 184–192.

Wilkinson, S. R. and Kelly, J. M. (2003). The role of glutathione peroxidases in trypanosomatids. *Biological Chemistry* **384**, 517–525.

Wilkinson, S. R., Meyer, D. J. and Kelly, J. M. (2000). Biochemical characterization of a trypanosome enzyme with glutathione-dependent peroxidase activity. *Biochemical Journal* **352**, 755–761.

Wilkinson, S. R., Prathalingam, S. R., Taylor, M. C., Ahmed, A., Horn, D. and Kelly, J. M. (2006). Functional characterisation of the iron superoxide dismutase gene repertoire in *Trypanosoma brucei*. *Free Radical Biology and Medicine* **40**, 198–209.

Wilson, R. J., Williamson, D. H. and Preiser, P. (1994). Malaria and other Apicomplexans: the "plant" connection. *Infectious Agents and Disease* **3**, 29–37.

Xu, P., Widmer, G., Wang, Y., Ozaki, L. S., Alves, J. M., Serrano, M. G., Puiu, D., Manque, P., Akiyoshi, D., Mackey, A. J., Pearson, W. R., Dear, P. H., Bankier, A. T., Peterson, D. L., Abrahamsen, M. S., Kapur, V., Tzipori, S. and Buck, G. A. (2004). The genome of *Cryptosporidium hominis*. *Nature* **431**, 1107–1112.

Yu, Y., Zhang, H. and Zhu, G. (2010). Plant-type trehalose synthetic pathway in *Cryptosporidium* and some other apicomplexans. *PLoS ONE* **5**, e12593.